



RESEARCH LETTER

10.1002/2014GL060301

Key Points:

- Unique coordinated observations by imagers, radars, and DMSP are presented
- A day-night coupling via a localized flow channel was identified
- Coupling between dayside and nightside reconnection was suggested

Supporting Information:

- Readme
- Figure S1
- Figure S2
- Movie S1

Correspondence to:

Y. Nishimura,
toshi@atmos.ucla.edu

Citation:

Nishimura, Y., et al. (2014), Day-night coupling by a localized flow channel visualized by polar cap patch propagation, *Geophys. Res. Lett.*, *41*, 3701–3709, doi:10.1002/2014GL060301.

Received 22 APR 2014

Accepted 14 MAY 2014

Accepted article online 15 MAY 2014

Published online 2 JUN 2014

Day-night coupling by a localized flow channel visualized by polar cap patch propagation

Y. Nishimura¹, L. R. Lyons¹, Y. Zou¹, K. Oksavik^{2,3}, J. I. Moen^{3,4}, L. B. Clausen⁴, E. F. Donovan⁵, V. Angelopoulos⁶, K. Shiokawa⁷, J. M. Ruohoniemi⁸, N. Nishitani⁷, K. A. McWilliams⁹, and M. Lester¹⁰

¹Department of Atmospheric and Oceanic Sciences, University of California, Los Angeles, California, USA, ²Birkeland Centre for Space Science, Department of Physics and Technology, University of Bergen, Bergen, Norway, ³Department of Geophysics, University Centre in Svalbard, Longyearbyen, Norway, ⁴Department of Physics, University of Oslo, Oslo, Norway, ⁵Department of Physics and Astronomy, University of Calgary, Calgary, Alberta, Canada, ⁶Department of Earth, Planetary and Space Sciences, University of California, Los Angeles, California, USA, ⁷Solar-Terrestrial Environment Laboratory, Nagoya University, Nagoya, Japan, ⁸Department of Electrical and Computer Engineering, Virginia Polytechnic Institute and State University, Blacksburg, Virginia, USA, ⁹Institute of Space and Atmospheric Studies, University of Saskatchewan, Saskatoon, Saskatchewan, Canada, ¹⁰Department of Physics and Astronomy, University of Leicester, Leicester, UK

Abstract We present unique coordinated observations of the dayside auroral oval, polar cap, and nightside auroral oval by three all-sky imagers, two Super Dual Auroral Radar Network (SuperDARN) radars, and Defense Meteorological Satellite Program (DMSP)-17. This data set revealed that a dayside poleward moving auroral form (PMAF) evolved into a polar cap airglow patch that propagated across the polar cap and then nightside poleward boundary intensifications (PBIs). SuperDARN observations detected fast antisunward flows associated with the PMAF, and the DMSP satellite, whose conjunction occurred within a few minutes after the PMAF initiation, measured enhanced low-latitude boundary layer precipitation and enhanced plasma density with a strong antisunward flow burst. The polar cap patch was spatially and temporally coincident with a localized antisunward flow channel. The propagation across the polar cap and the subsequent PBIs suggests that the flow channel originated from dayside reconnection and then reached the nightside open-closed boundary, triggering localized nightside reconnection and flow bursts within the plasma sheet.

1. Introduction

Plasma convection in the magnetosphere-ionosphere system can be thought of as composed of large-scale slower two-cell convection punctuated by dynamic mesoscale fast flows of the order of 100 km size in the ionosphere. Those flow channels are often seen in the high-latitude ionosphere near the cusp [Oksavik et al., 2004, 2005; Rinne et al., 2007; Moen et al., 2008] and in the nightside auroral oval [Lyons et al., 2012]. Dayside ionospheric flow channels are associated with auroral intensifications and subsequent poleward moving auroral forms (PMAFs), which are understood as ionospheric signatures of localized dayside magnetic reconnection events [Sandholt et al., 2003; Carlson et al., 2006; McWilliams et al., 2000]. PMAFs are associated with high-density *F* region plasma called polar cap airglow patches that continue propagating poleward after PMAFs decay [Lorentzen et al., 2010]. Ionospheric flow channels in the nightside auroral oval are associated with poleward boundary intensifications (PBIs), their subsequent equatorward propagation as auroral streamers, and with major geomagnetic disturbances such as substorms [Nishimura et al., 2010a]. The PBIs and streamers are the ionospheric manifestation of nightside reconnection and plasma sheet flow bursts [Sergeev et al., 2000], which are a critical component of nightside plasma transport [Angelopoulos et al., 1994]. However, the process that initiates nightside reconnection and plasma sheet flow bursts has remained elusive. Dayside and nightside flow channels observed in the ionosphere have similarities in terms of their bursty nature and their associations with localized reconnection within the large-scale convection system. These similarities open the question of whether dayside and nightside flow channels are related to each other, which would give a possibility that dayside flow channels may be an important driver of nightside flow channels.

PMAF and airglow patch observations are usually limited to the dayside polar region, and they rarely have been observed to extend deep into the polar cap except for large-scale tongues of ionization, which seem to follow large-scale convection velocities [e.g., Foster et al., 2005; Hosokawa et al., 2010; Thomas et al., 2013]. Nightside PBIs and streamers have been related to mesoscale flow enhancements within the polar cap

[*de la Beaujardière et al., 1994; Nishimura et al., 2010b; Lyons et al., 2011; Zou et al., 2014*], indicating that fast flows crossing the nightside open-closed field line boundary often trigger tail reconnection, giving energetic electron precipitation toward the ionosphere near the polar cap boundary and illuminating PBIs. Such connections can also be inferred from nightside polar cap patches that have been observed to drift toward the auroral poleward boundary and connect to PBIs [*Lorentzen et al., 2004; Moen et al., 2007; Nishimura et al., 2013*]. However, these nightside observations were limited by spatial coverage that extended only up to the vicinity of the magnetic pole.

Visualization of plasma transport over large distances has been attempted using localized density enhancements associated with polar cap patches measured by the Super Dual Auroral Radar Network (SuperDARN) radars [*Oksavik et al., 2010*] and the GPS network [*Zhang et al., 2013*]. They showed propagation of high-density plasma from the dayside ionosphere reaching the nightside, suggesting that polar cap patches forming on the dayside can propagate all the way across the polar cap. Their observations were, however, limited by coverage gaps near the magnetic pole, and no distinction was made between large-scale and mesoscale flows. Also, the lack of auroral imaging did not allow finding the influence of the patch on the nightside aurora.

Optical observations in the 630.0 nm wavelength are important for detecting patch propagation with larger spatial coverage as well as examining patch initiation in the dayside auroral oval and consequence in the nightside auroral oval. Simultaneous ground-based optical observations in the 630.0 nm wavelength that cover dayside, polar cap, and nightside have been very difficult due to the limited number of days sufficiently near the winter solstice and unfavorable sky conditions. *Sandholt et al. [1986]* presented simultaneous observations of a dayside imager and a nightside meridian-scanning photometer. They treated dayside and nightside signatures separately, however, and did not discuss their optical connections. *Hosokawa et al. [2014]* used two imagers for studying the patch size, but their imager data were limited by sunlight contamination within the dayside portion of the imager field of view (FOV).

In the present paper, we report simultaneous observations of the dayside, polar cap, and nightside polar region by three all-sky imagers (ASIs), two SuperDARN radars, and a Defense Meteorological Satellite Program (DMSP) satellite. These instruments provided a nearly continuous optical sequence of a PMAF and polar cap patch propagating across the polar cap from the dayside polar region toward the nightside auroral oval. The patch in the nightside polar cap was associated with a narrow flow channel, indicating that fast mesoscale flows initiating on the dayside transported the enhanced density over a limited longitude range toward the nightside auroral oval. Then PBIs occurred along the nightside auroral poleward boundary, suggesting that nightside reconnection and plasma sheet flow bursts were triggered by the fast flow channels.

2. Data Set

The ASI at Ny-Ålesund (NYA, 78.9°N and 11.9°E geographic, 75.9°N and 127.9°E geomagnetic, magnetic local time (MLT) = UT + 3 h) detects aurora in 557.7 and 630.0 nm wavelength above 20° elevation in 30 s resolution. This camera has been used widely for detecting dayside aurora and polar cap patches [*Moen et al., 2012*]. The ASI at Resolute Bay (RES, 74.7°N and 265.1°E geographic, 82.8°N and 56.4°W geomagnetic, MLT = UT + 7 h) also provides 557.7 and 630.0 nm wavelength data with 2 min resolution and at all elevations above the horizon [*Shiokawa et al., 1999*]. The Time History of Events and Macroscale Interactions during Substorms (THEMIS) ASI at Rankin Inlet (RKN, 62.8°N and -93.11°E geographic, 71.6°N and 31.2°W geomagnetic) measures aurora in white light in 3 s cadence [*Angelopoulos, 2008; Mende et al., 2008*]. When mapping ASI data to the sky, 557.7 nm and white light data were mapped to 110 km altitude (corresponding to ~10 keV electron precipitation), and 630.0 nm data were mapped to 250 km altitude. More details of RES and THEMIS ASI imager data processing are described in *Nishimura et al. [2013]*.

Ionospheric flows were obtained from the SuperDARN radars at Hankasalmi (HAN, 62.3°N and 26.6°E geographic, 59.2°N and 115.9°E geomagnetic) and Rankin Inlet (RKN, colocated with the THEMIS ASI) [*Chisham et al., 2007*]. Ground-scatter echoes were removed. Their measurements give line of sight (LOS) flows but not information on flows perpendicular to the radar beam directions. The DMSP-17 satellite provides precipitating particles, plasma density, and cross-track plasma flows at 850 km altitude on the dayside near the NYA imager FOV.

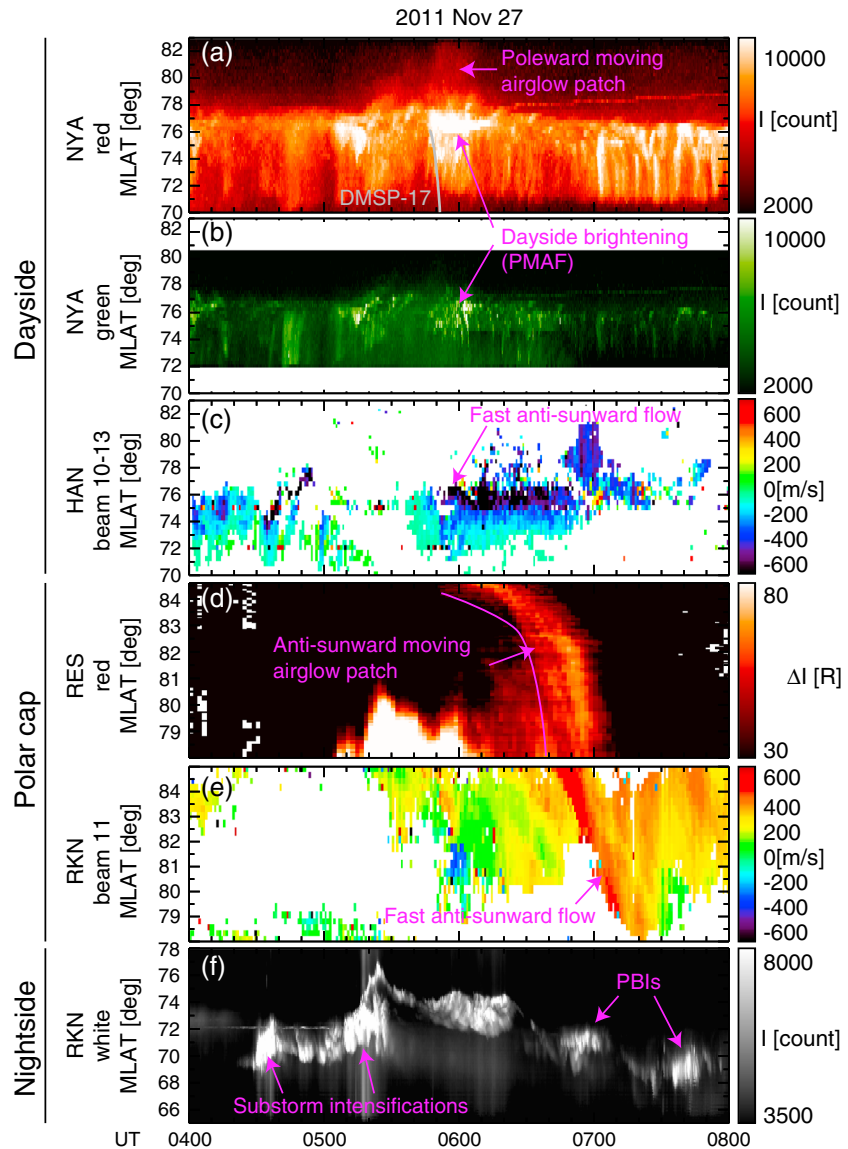


Figure 1. Time series of the (a) 630.0 and (b) 557.7 nm NYA imager keograms using all longitudes, (c) HAN radar LOS flow keogram from beams 10–13, (d) RES 630.0 nm imager keogram along the line shown in Figure 2a, (e) RKN radar LOS flow keogram from beam 11, and (f) RKN white light imager keogram. Positive flows are directed toward the radar. The DMSP orbit is drawn in Figure 1a in gray.

3. Results

Figure 1 shows a time series of the imager and radar data as north-south keograms at 4–8 UT on 27 November 2011. The NYA imager was located in the prenoon sector and detected the poleward boundary of the dayside auroral oval at $\sim 78^\circ$ magnetic latitude (MLAT) at the beginning of this time interval. The oval at 630.0 nm was steady and moderately intensified at 4–5 UT. Soon after 0500 UT, the poleward edge of the auroral oval showed a weak brightening followed by poleward propagation that appeared to stop at $\sim 80^\circ$ MLAT. A stronger brightening occurred at 0546 UT, followed by rapid poleward propagation of a faint emission that reached the high-latitude edge of the imager FOV. The 557.7 nm data also show this brightening along the poleward boundary and a small ($\sim 1^\circ$) poleward extension. In contrast, no significant 557.7 nm emission was seen beyond 78° MLAT. This contrast indicates that the brightening along the poleward boundary and part of the poleward propagation is a PMAF associated with electron precipitation, and the subsequent poleward propagation dominated by

630.0 nm wavelength is a typical signature of a polar cap airglow patch. The intensification lasted for ~ 30 min, and the auroral condition then returned to the preintensification level.

The interplanetary magnetic field (IMF) B_z from the OMNI database and four satellites in the solar wind are shown in Figure S1 in the supporting information. While the OMNI data indicate southward IMF throughout the period of interest (4–8 UT), the polarity of the B_z component differed significantly between the available upstream satellite monitors, probably due to small-scale structure in the solar wind. In particular, the ACE, TH-B, and Geotail satellites measured northward IMF albeit with inconsistent timings; however, these all lay on the duskside under positive V_y conditions. While none of the solar wind vectors measured at the satellites was directed toward the subsolar magnetopause, the OMNI propagation analysis, which combines multiple-satellite data with realistic propagation, represents the best estimate of the IMF conditions that prevailed there and is primarily due to Wind observations, which showed negative B_z . Moreover, the AE index showed small excursions consistent with negative B_z after 4 UT followed by a steady increase. The large-scale pattern of convection inferred from SuperDARN radar observations depicted in Figure S2 for 2 min scans that span the primary period of interest shows moderately enhanced flows of the two-cell type extending to about 65° MLAT with sustained antisunward flows across the polar cap. These features indicate that the effective IMF at the magnetopause was in fact negative B_z , consistent with the OMNI analysis and AE. Thus, we infer that significant solar wind driving occurred during the PMAF and the subsequent airglow patch and flow channel propagated across the polar cap. Note, however, that this approach does not tell us the stability of the IMF so that the IMF could have had substantial fluctuations and thus may not have been stably southward throughout the entire period.

The HAN radar shares the FOV with the NYA imager FOV, as shown in Figure 2. Beams with the strongest flows during this time interval (10–13) were selected, and maximum values were calculated when creating the combined keogram shown in Figure 1c. The flow magnitude was small (~ 100 m/s) between 0500 and 0544 UT. Then the flow speed near the auroral poleward boundary increased to ~ 300 m/s directed away from the radar (approximately antisunward) at 0545 UT and further to ~ 900 m/s at 0556 UT. The initiation of the enhanced flows coincided well with the initiation of the PMAF. Although the echoes were initially confined to the equatorward side of the PMAF, they later extended to higher latitudes.

The RES imager was located in the nightside polar cap, and its keogram (Figure 1d) shows an isolated polar cap patch that propagated antisunward. Based on its location, timing, and isolated nature, this nightside polar cap patch is likely a continuation of the dayside polar cap patch seen in Figure 1a. The propagation speed change at $\sim 83^\circ$ MLAT is an apparent effect because the keogram line (drawn in Figure 2a) has a large angle to the north-south direction at higher latitudes. The RKN radar beam 11, which goes through the airglow patch, detected an antisunward fast flow channel at the same time as the airglow patch (Figure 1e). The flow speed (~ 500 m/s) is roughly consistent with the optical propagation speed ($\sim 3^\circ$ MLAT per 10 min), as can be seen from the similar tilt angles in the keograms.

This airglow patch reached the equatorward edge of the RES imager FOV, and then two PBIs were seen by the RKN imager (Figure 1f). The first PBI occurred ~ 7 min after the airglow reached the equatorward boundary of the RES imager FOV. Although the white light imager is not capable of detecting airglow emissions, based on this timing, this PBI appears to occur when the airglow patch approaches the airglow patch and flow channel in a similar way as in the *Nishimura et al.* [2013] events. The airglow patch continued propagating equatorward and still existed at the time of the second PBI, although the azimuthal motion of the patch carried it away from the keogram meridian before 0710 UT (seen in the Figure 2 snapshots). This multistation observation shows a link between the dayside and nightside auroral activity via a localized flow channel and an airglow patch. We do not discuss the substorm intensifications that occurred before these PBIs. Although polar cap emissions were present before the substorm, the NYA imager at that time was too far from noon to identify a connection to dayside aurora.

The spatial structure of the optical and radar flow signatures can be seen in the 2-D snapshots in Figures 2 (630.0 nm wavelength of NYA and RES and RKN) and 3 (557.7 nm wavelength of NYA and RES and RKN). The whole sequence of Figure 2 is given in Movie S1 in the supporting information. At the time of Figure 2a, the auroral oval in the prenoon sector seen by the NYA imager was steady and had moderate intensity. The poleward boundary of the auroral emission (polar cap boundary) is traced by the gray line. The poleward boundary at this time was located at a quite high latitude. This is because of the auroral poleward expansion

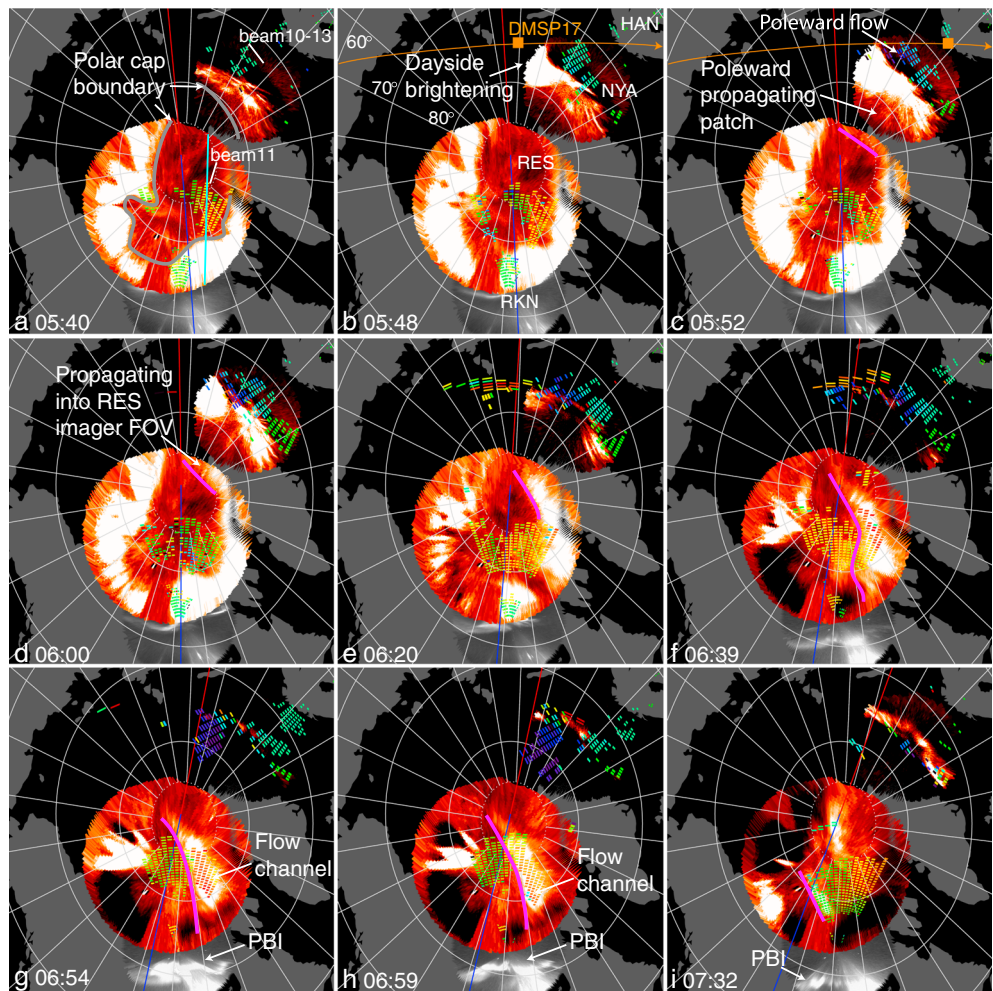


Figure 2. Snapshots of imager and radar data. Imagers shown are NYA (630.0 nm), RES (630.0 nm), and RKN (white light). The LOS flows from SuperDARN radars (HAN and RKN) are color coded using the color bar shown in the bottom right corner. The pink lines mark the duskward edge of the airglow patch. The light blue line in Figure 2a indicates the keogram slice used in Figure 1e. The red and blue lines mark the magnetic noon and midnight meridians. The magnetic latitude and longitude contours are given every 10° and 15°. The DMSP-17 footprint is shown in an orange square, and the satellite track is shown in orange.

during the substorm expansion phase that occurred before this time, and we checked that the poleward expanding arc location seen by all available THEMIS ASIs falls within the poleward boundary emission seen in Figure 2. The echoes from the HAN radar did not show any enhanced flows. A sudden auroral brightening occurred near the duskside edge of the NYA imager FOV at ~11 MLT (Figure 2b) and then expanded poleward as a PMAF and also downward (Figure 2c). The HAN radar detected enhanced flows directed away from the radar just near the PMAF, as identified in Figure 2c. The RES imager and RKN radar did not observe any substantial change up to this time.

The PMAF was followed by a polar cap airglow patch (Figure 2c) that moved into the RES imager FOV (Figures 2d and 2e). The duskside edge of the airglow patch is marked by the pink line. The lack of corresponding emissions in the 557.7 nm wavelength (Figures 3c–3e) indicates again that this is not a polar cap arc but an airglow patch. Although the preexisting auroral emissions obscured the antisunward edge of this airglow patch, the entire shape was seen when the auroral emission moved equatorward, and the airglow patch became detached entirely from the auroral oval (Figure 2f). The airglow patch then moved well into the RKN radar echo coverage in the nightside polar cap, and the whole azimuthal extent of the patch was covered by the available echoes at the times of Figures 2g and 2h. Fast flows directed toward the radar

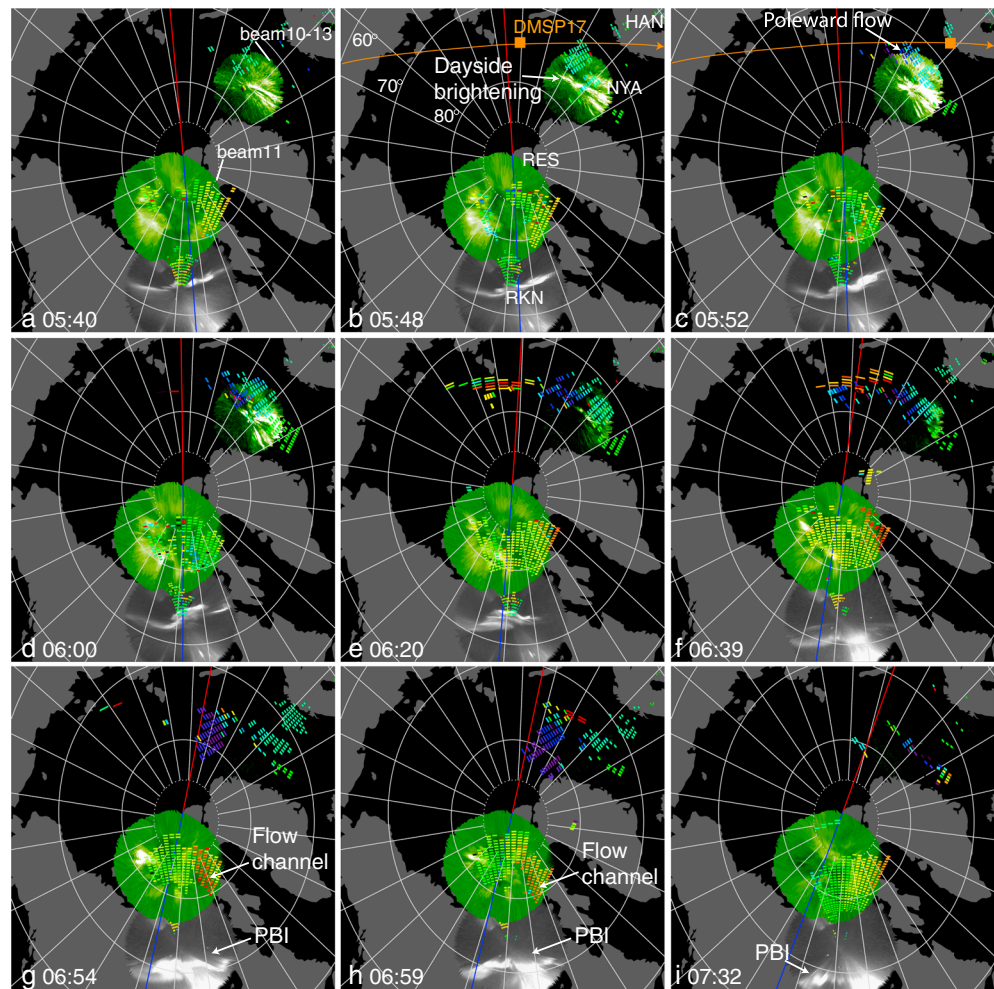


Figure 3. Same as Figure 2 but using the 557.7 nm data from NYA and RES.

were seen on the airglow patch and were confined to the patch azimuthal width. This indicates that the fast flows formed an azimuthally narrow flow channel aligned with the patch (The channel shape is seen more clearly in Figure 3.). In spite of the LOS measurements, the sharp gradient of the LOS flow speed at the dawnside and duskside edges of the patch and flow continuity suggests that the flows are directed along the patch orientation and antisunward. Polar cap convection during this event was dominated by this narrow flow channel, which had flows twice as fast as the large-scale background flow seen outside the channel.

By the time of the Figure 2f snapshot, the antisunward edge of the airglow patch reached the nightside edge of the RES imager FOV. A PBI was then seen within the RKN imager FOV near the meridian of the airglow and flow channel (Figures 2g and 2h). The airglow patch moved farther equatorward and duskward, and the RKN imager shows that another PBI then developed near the airglow meridian in the RKN imager FOV (Figure 2i). Bright emissions in the 557.7 nm wavelength are not polar cap auroras but emissions in the auroral oval and polar cap gravity waves.

At the time of the dayside auroral brightening, the DMSP-17 satellite passed just to the east of the NYA imager FOV, as shown in Figure 2b. Since this is a Northern Hemisphere pass, our field line mapping using the International Geomagnetic Reference Field magnetic field model is accurate. Although the azimuthal extent of the auroral brightening is unknown, the enhanced electron and ion precipitation of the low-latitude boundary layer type [Newell and Meng, 1994] seen at the time of the brightening (0548–49 UT, Figure 4g) suggests that the satellite passed over the brightening. A very fast flow burst exceeding 4000 m/s together with an enhanced plasma density and large upflow was detected within this precipitation region. The flow

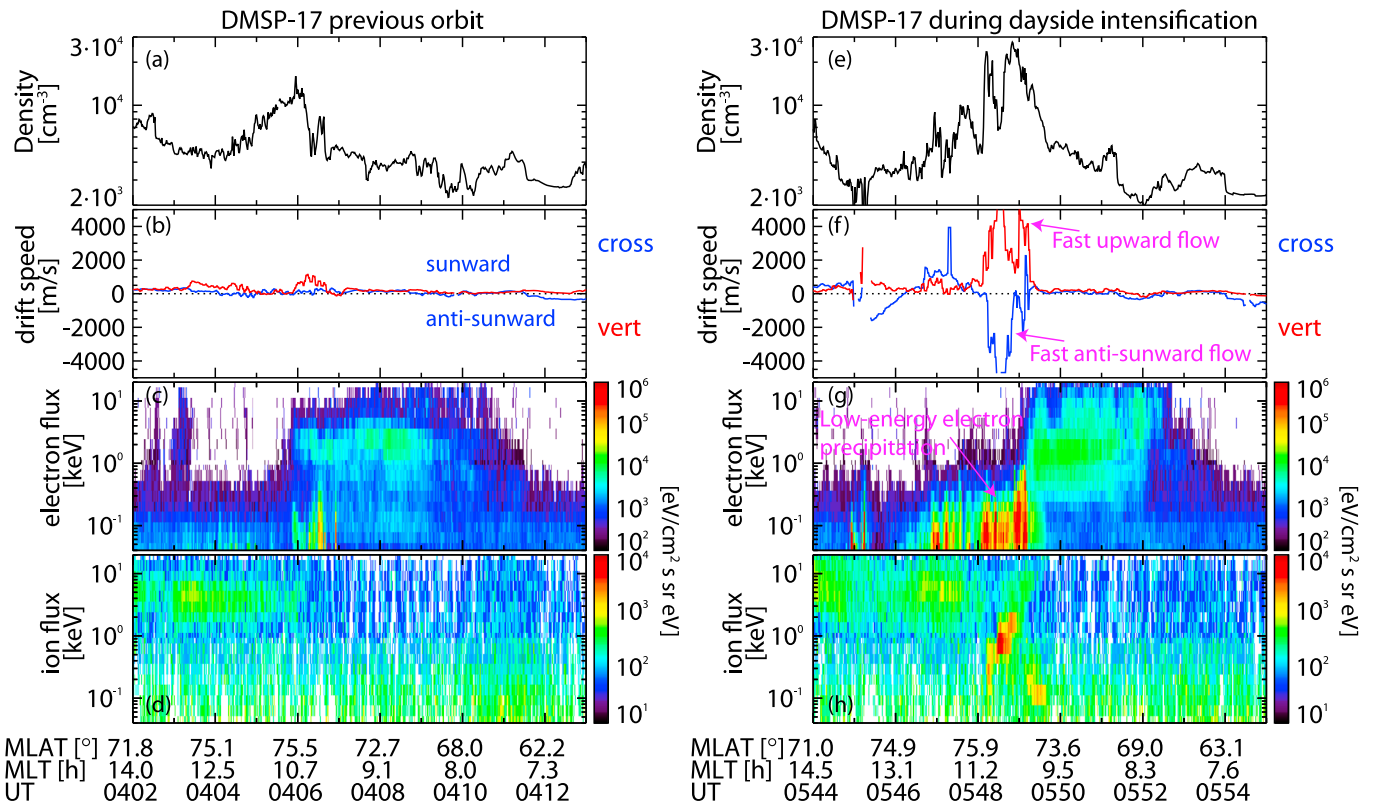


Figure 4. DMSP-17 satellite data before and during the dayside auroral brightening. Shown are the (a and e) plasma density, (b and f) drift speed, (c and g) electron flux, and (d and h) ion flux.

was directed antisunward and across the satellite path. Such a fast flow channel and enhanced precipitation were not seen on the previous orbit about 100 min before (Figures 4a–4d), when the dayside auroral oval based on the NYA imager data was steady and only showed moderate intensity (Figure 1a). The existence of the fast flow in association with the enhanced precipitation is consistent with the fast antisunward flow measured by the HAN radar. The radar flow magnitude is much smaller, but this could be due to the different LOS directions and measured locations. The large upflow collocated with the antisunward flow suggests that the *F* region plasma was lifted up, giving a longer lifetime of the high-density region to propagate across the polar cap before quenching by recombination. Thus, the DMSP data support the idea that a fast flow channel formed in association with enhanced density and precipitation along the dayside auroral poleward boundary and that the flow channel propagated deep into the polar cap together with the enhanced plasma density, which can be seen as the airglow patch in the 630.0 nm data.

4. Conclusion

We have presented extraordinary simultaneous observations by ground-based auroral imagers, SuperDARN radars, and a satellite that cover the polar ionosphere on the dayside, in the polar cap, and on the nightside during a transient disturbance in the ionosphere. The optical data provide a nearly continuous view of a sequence that starts from a dayside PMAF and is followed by a polar cap patch propagating across the polar cap and then nightside PBIs. Although we cannot determine what triggers the PMAF, the DMSP observations show that the PMAF was associated with enhanced precipitation and density and fast antisunward flows that are consistent with the poleward propagation of the optical signature. A flow enhancement associated with the PMAF was also seen by SuperDARN. The antisunward enhanced flow extended deep into the polar cap as a longitudinally narrow channel aligned with the antisunward propagating airglow patch, which continued propagating toward the nightside polar cap boundary and precedes the PBIs.

This optical and flow sequence provides observational evidence that transient flows and airglow patches initiating on the dayside can propagate across the polar cap and impact nightside auroral intensifications. The existence of the narrow flow channel in the nightside polar cap in association with the airglow patch indicates that the dayside mesoscale flows propagate deep into the polar cap without diffusing away and that the polar cap patch was transported by the enhanced flow channel rather than by slow, large-scale convection. Considering that electric fields between the ionosphere and magnetosphere can communicate in a much shorter time scale (of the order of minutes) than the patch propagation across the polar cap (~hour), the fast flow channel in the polar cap propagating toward the nightside polar cap boundary likely represents a flow channel in the lobe propagating toward the nightside plasma sheet. Thus, the connection to the PBIs suggests that such flow channels reaching the nightside open-closed boundary trigger localized reconnection and lead to plasma sheet flow bursts.

The PMAF and the associated precipitation and fast flows on the dayside can be attributed to enhanced reconnection at the magnetopause under the southward or fluctuating IMF, and subsequent poleward propagation of newly reconnected flux tubes [Sandholt *et al.*, 2003; Carlson *et al.*, 2006], although the precise cause of this dayside transient is not clear from our data set. Another issue to note is that not all PMAFs are followed by patches that propagate deep into the polar cap. The earlier PMAF and airglow patch, seen at 0505–0540 UT in Figure 1a, disappeared before reaching the RES imager FOV. While this might be related to the lack of fast flows (Figure 1c), further investigations are needed to understand the conditions that lead to patches propagating deep into the polar cap.

Acknowledgments

This work was supported by NASA grants NNX12AJ57G, NNX09AI06G, and NASS-02099, NSF grants AGS-1101903, AGS-1042255, AGS-1242356, and AGS-1004736, and CSA contract 9F007-046101. The optical observation at Resolute Bay was supported by the NSF grant ATM-0608577 and a grant-in-aid for Scientific Research (16403007, 19403010, and 20740282) of MEXT, Japan. The DMSP data are maintained by the Air Force Research Laboratory and Applied Physics Laboratory at Johns Hopkins University. K.O., J.I.M., and L.B.N.C. acknowledge financial support by the Research Council of Norway. L.B.N.C. and the imager at NYA are supported by Norges forskningsrad under contract 230935. We thank K. Hosokawa for useful discussions. Data of the THEMIS ASI, RES imager, NYA imager, and SuperDARN can be accessed from <http://themis.ssl.berkeley.edu/>, <http://gwave.ice.uec.ac.jp/cgi-bin/hosokawa/resolute/resolute.cgi>, <http://tid.uio.no/plasma/aurora/>, and <http://vt.superdarn.org/>. The solar wind data were obtained from the CDAWeb. The DMSP data can be provided from the author upon request.

The Editor thanks two anonymous reviewers for their assistance in evaluating this paper.

References

- Angelopoulos, V. (2008), The THEMIS mission, *Space Sci. Rev.*, *321*, 47.
- Angelopoulos, V., *et al.* (1994), Statistical characteristics of bursty bulk flow events, *J. Geophys. Res.*, *99*, 21,257–21,280, doi:10.1029/94JA01263.
- Carlson, H. C., J. Moen, K. Oksavik, C. P. Nielsen, I. W. McCrea, T. R. Pedersen, and P. Gallop (2006), Direct observations of injection events of subauroral plasma into the polar cap, *Geophys. Res. Lett.*, *33*, L05103, doi:10.1029/2005GL025230.
- Chisham, G., *et al.* (2007), A decade of the Super Dual Auroral Radar Network (SuperDARN): Scientific achievements, new techniques and future directions, *Surv. Geophys.*, *28*(1), 33–109.
- de la Beaujardière, O., L. R. Lyons, J. M. Ruohoniemi, E. Friis-Christensen, C. Danielsen, F. J. Rich, and P. T. Newell (1994), Quiet-time intensifications along the poleward auroral boundary near midnight, *J. Geophys. Res.*, *99*(A1), 287–298, doi:10.1029/93JA01947.
- Foster, J. C., *et al.* (2005), Multiradar observations of the polar tongue of ionization, *J. Geophys. Res.*, *110*, A09S31, doi:10.1029/2004JA010928.
- Hosokawa, K., T. Tsugawa, K. Shiokawa, Y. Otsuka, N. Nishitani, T. Ogawa, and M. R. Hairston (2010), Dynamic temporal evolution of polar cap tongue of ionization during magnetic storm, *J. Geophys. Res.*, *115*, A12333, doi:10.1029/2010JA015848.
- Hosokawa, K., S. Taguchi, K. Shiokawa, Y. Otsuka, Y. Ogawa, and M. Nicolls (2014), Global imaging of polar cap patches with dual airglow imagers, *Geophys. Res. Lett.*, *41*, 1–6, doi:10.1002/2013GL058748.
- Lorentzen, D. A., N. Shumilov, and J. Moen (2004), Drifting airglow patches in relation to tail reconnection, *Geophys. Res. Lett.*, *31*, L02806, doi:10.1029/2003GL017785.
- Lorentzen, D. A., J. Moen, K. Oksavik, F. Sigernes, Y. Saito, and M. G. Johnsen (2010), In situ measurement of a newly created polar cap patch, *J. Geophys. Res.*, *115*, A12323, doi:10.1029/2010JA015710.
- Lyons, L. R., Y. Nishimura, H.-J. Kim, E. Donovan, V. Angelopoulos, G. Sofko, M. Nicolls, C. Heinselman, J. M. Ruohoniemi, and N. Nishitani (2011), Possible connection of polar cap flows to pre- and post-substorm onset PBIs and streamers, *J. Geophys. Res.*, *116*, A12225, doi:10.1029/2011JA016850.
- Lyons, L. R., Y. Nishimura, X. Xing, Y. Shi, M. Gkioulidou, C.-P. Wang, H.-J. Kim, S. Zou, V. Angelopoulos, and E. Donovan (2012), Auroral disturbances as a manifestation of interplay between large-scale and mesoscale structure of magnetosphere-ionosphere electrodynamic coupling, in *Auroral Phenomenology and Magnetospheric Processes: Earth and Other Planets*, *Geophys. Monogr. Ser.*, vol. 197, edited by A. Keiling *et al.*, pp. 193–204, AGU, Washington, D. C.
- McWilliams, K. A., T. K. Yeoman, and G. Provan (2000), A statistical survey of dayside pulsed ionospheric flows as seen by the CUTLASS Finland HF radar, *Ann. Geophys.*, *18*, 445–453.
- Mende, S. B., *et al.* (2008), The THEMIS array of ground-based observatories for the study of auroral substorms, *Space Sci. Rev.*, *141*, 357–387.
- Moen, J., N. Gulbrandsen, D. A. Lorentzen, and H. C. Carlson (2007), On the MLT distribution of F region polar cap patches at night, *Geophys. Res. Lett.*, *34*, L14113, doi:10.1029/2007GL029632.
- Moen, J., Y. Rinne, H. C. Carlson, K. Oksavik, R. Fujii, and H. Opgenoorth (2008), On the relationship between thin Birkeland current arcs and reversed flow channels in the winter cusp/cleft ionosphere, *J. Geophys. Res.*, *113*, A09220, doi:10.1029/2008JA013061.
- Moen, J., H. C. Carlson, Y. Rinne, and Å. Skjæveland (2012), Multi-scale features of solar terrestrial coupling in the cusp ionosphere, *J. Atmos. Sol. Terr. Phys.*, *87*–88, 11–19.
- Newell, P. T., and C.-I. Meng (1994), Ionospheric projections of magnetospheric regions under low and high solar wind pressure conditions, *J. Geophys. Res.*, *99*(A1), 273–286, doi:10.1029/93JA02273.
- Nishimura, Y., L. Lyons, S. Zou, V. Angelopoulos, and S. Mende (2010a), Substorm triggering by new plasma intrusion: THEMIS all-sky imager observations, *J. Geophys. Res.*, *115*, A07222, doi:10.1029/2009JA015166.
- Nishimura, Y., *et al.* (2010b), Preonset time sequence of auroral substorms: Coordinated observations by all-sky imagers, satellites, and radars, *J. Geophys. Res.*, *115*, A00108, doi:10.1029/2010JA015832.
- Nishimura, Y., L. R. Lyons, K. Shiokawa, V. Angelopoulos, E. F. Donovan, and S. B. Mende (2013), Substorm onset and expansion phase intensification precursors seen in polar cap patches and arcs, *J. Geophys. Res. Space Physics*, *118*, 2034–2042, doi:10.1002/jgra.50279.

- Oksavik, K., J. Moen, and H. C. Carlson (2004), High-resolution observations of the small-scale flow pattern associated with a poleward moving auroral form in the cusp, *Geophys. Res. Lett.*, *31*, L11807, doi:10.1029/2004GL019838.
- Oksavik, K., J. Moen, H. C. Carlson, R. A. Greenwald, S. E. Milan, M. Lester, W. F. Denig, and R. J. Barnes (2005), Multi-instrument mapping of the small-scale flow dynamics related to a cusp auroral transient, *Ann. Geophys.*, *23*, 2657–2670.
- Oksavik, K., V. L. Barth, J. Moen, and M. Lester (2010), On the entry and transit of high-density plasma across the polar cap, *J. Geophys. Res.*, *115*, A12308, doi:10.1029/2010JA015817.
- Rinne, Y., J. Moen, K. Oksavik, and H. C. Carlson (2007), Multi-instrument mapping of the small-scale flow dynamics related to a cusp auroral transient, *J. Geophys. Res.*, *112*, A10313, doi:10.1029/2007JA012366.
- Sandholt, P. E., C. S. Deehr, A. Egeland, B. Lybakk, R. Viereck, and G. J. Romick (1986), Signatures in the dayside aurora of plasma transfer from the magnetosheath, *J. Geophys. Res.*, *91*(A9), 10,063–10,079, doi:10.1029/JA091iA09p10063.
- Sandholt, P. E., C. J. Farrugia, W. F. Denig, S. W. H. Cowley, and M. Lester (2003), Spontaneous and driven cusp dynamics: Optical aurora, particle precipitation, and plasma convection, *Planet. Space Sci.*, *51*, 797–812.
- Sergeev, V. A., et al. (2000), Multiple-spacecraft observation of a narrow transient plasma jet in the Earth's plasma sheet, *Geophys. Res. Lett.*, *27*, 851–854, doi:10.1029/1999GL010729.
- Shiokawa, K., Y. Katoh, M. Satoh, M. K. Ejiri, T. Ogawa, T. Nakamura, T. Tsuda, and R. H. Wiens (1999), Development of optical mesosphere thermosphere imagers (OMTI), *Earth Planets Space*, *51*, 887–896.
- Thomas, E. G., J. B. H. Baker, J. M. Ruohoniemi, L. B. N. Clausen, A. J. Coster, J. C. Foster, and P. J. Erickson (2013), Direct observations of the role of convection electric field in the formation of a polar tongue of ionization from storm enhanced density, *J. Geophys. Res. Space Physics*, *118*, 1180–1189, doi:10.1002/jgra.50116.
- Zhang, Q.-H., et al. (2013), Direct observations of the evolution of polar Cap ionization patches, *Science*, *339*, 1597–1600.
- Zou, Y., Y. Nishimura, L. R. Lyons, E. F. Donovan, J. M. Ruohoniemi, N. Nishitani, and K. A. McWilliams (2014), Statistical relationships between enhanced polar cap flows and PBIs, *J. Geophys. Res. Space Physics*, *119*, 151–162, doi:10.1002/2013JA019269.